Atlantis Highlights in Engineering, volume 6

14th International Renewable Energy Storage Conference 2020 (IRES 2020)

Performance Evaluation of a Cylindrical PEM Fuel Cell and the Stack

Suseendiran S. Ravichandran
Department of Chemical Engineering
Indian Institute of Technology Madras
Chennai, India
srsuseendiran@gmail.com

Amit C. Bhosale
Department of Hydro and Renewable Energy
Indian Institute of Technology Roorkee
Roorkee, India
achbhosale@hre.iitr.ac.in

Ramya Ramkumar
Department of Chemical Engineering
Indian Institute of Technology Madras
Chennai, India
ramya.iitm@gmail.com

Gowri Mohandass
Department of Chemical Engineering
Indian Institute of Technology Madras
Chennai, India
gowrimohandass94@gmail.com

Raghunathan Rengasamy
Department of Chemical Engineering
Indian Institute of Technology Madras
Chennai, India
raghur@iitm.ac.in

Suman Roy Choudhury
Naval Materials Research Laboratory
Defense Research and Development Organization
Ambernath, India
sumansrc1@gmail.com

***Abstract*— Air-breathing fuel cells, due to their ability of using oxygen directly from air, have the potential to emerge as a primary power source for various applications. Cylindrical fuel cells offer the advantage of higher gravimetric and volumetric power densities compared to conventional planar fuel cells. In the present study, the durability of single cylindrical cell is tested based on a new European driving cycle and the cell is shown to be stable for more than 200 h of operation at different current densities. The decrease in the performance is observed to be the result of increase in membrane resistance rather than catalyst degradation or hydrogen crossover. Furthermore, the performance of a stack of 16 cylindrical fuel cells is evaluated at different relative humidities and temperatures of air on the cathode side. The effect of cell positioning on the stack performance in terms of deficiency of oxygen is also studied. Both relative humidity and temperature are observed to have an effect on the durability of the stack. Increment in the temperature of air is also seen to upset the performance of the stack. Higher relative humidity (~80%) and lower temperature (~35 ºC) are observed to stabilize the stack in terms of performance and durability on a time scale of more than 2 h.**

Keywords— Fuel cells, Air-breathing, cylindrical, temperature, humidity, durability

I. INTRODUCTION

With increase in the energy demand globally and the depletion of conventional energy resources, other possible sources of energy such as solar, wind, geothermal, nuclear etc. [1], have been explored. The energy produced by the renewable energy sources like solar and wind are intermittent in nature and hence batteries are required to store this energy [2]. Lead-acid batteries were conventionally employed for storing the solar or wind energy which are being replaced by lithium-ion batteries in recent times [3]. Vanadium Redox Flow Batteries (VRFB) are also being considered because they allow decoupling of power and energy [4]. Supercapacitors are another class of energy storage devices which are employed when very high power must be drawn in a very short time [5]. Polymer electrolyte membrane fuel cell (PEMFC) is an energy conversion device which has the potential to bring the benefits of renewable energy to the transportation applications [6], [7]. The energy produced from renewable resources can be used to produce hydrogen from water. The hydrogen can then be consumed in a PEMFC to produce electricity with water as the only byproduct.

PEMFCs are traditionally made of anode, cathode and an ion conducting (mostly Nafion®) membrane in a planar arrangement. A stack of these individual cells assembled in series produces a high voltage and in parallel to produce high current. Researchers have focused on developing a single cell/stack [8], anode/cathode materials [9], [10], design [11], addition of catalysts [12] and various ion conducting membranes [13], [14] to improve the performance of the fuel cell. Their inherent abilities such as quick start, silent operation, high power density, environmental stability etc. have made them favourites among the other sources [15], [16]. However, cost and durability are still considered to be major barriers for such fuel cells' commercialization [17], [18].

Air-breathing PEMFCs offer more advantages over conventional ones (H_2/O_2 as fuel and oxidants) in the view of their lightweight features and less subsystems used with a corresponding slight compromise on the performance. The absence of oxygen cylinder, heat and water management systems make such air-breathing cells a preferred choice in applications such as portable power generation [19], space applications [20], underwater vehicles [21], automobiles etc. [22], [23]. Air circulation, however, is very important and decides the performance of the air-breathing cells [24]. Deryn Chu et al. [25] evaluated the effect of relative humidity (RH) and temperature of the air surrounding a stack of 6 cells. The group observed that humidity dominated the performance of the stack with least performance at RH<30% increasing rapidly afterwards. The temperature was also observed to influence the stack performance considerably. Tibor Fabian et al [26] experimentally found out the effect of ambient conditions on an air breathing cell operated in a dead-end mode. They observed the thermal plume's velocity to be an important factor that affects the cell performance. Furthermore, a temperature of 60 ℃ was found to be the transition temperature at which water removal due to evaporation equalled water generation in the cell.

Forced air breathing stacks of different capacity (50-1500 W) were tested for factors such as humidity, air flow, temperature etc. [27]. The stacks performed better and were stable for higher air flow rates and humidity. In order to make

the stack useful for portable applications, an 8 cell stack was extensively tested for different conditions mentioned earlier [28]. The stack temperature, when increased beyond 30 °C, dried the membrane thus adding to the ohmic losses. The maximum power produced was 10 W when operated at 333 mA/cm^2 with other factors maintained constant.

Cylindrical (also known as tubular) fuel cells, being very light weight compared to the conventional air breathing PEMFCs, offer higher volumetric and gravimetric power density [29], [30]. They are also proven to have reduced pressure losses than conventional ones [31]. Z. Saghali et al [32] numerically compared the designs of conical and cylindrical fuel cells and found that conical design had a superiority in terms of performance for higher conical angle. The group also highlighted that relative humidity influences the effectiveness of the shape proposed.

The durability of the cell is one of the limiting factors for fuel cells' commercialization. The U. S. Department of Energy (DOE) has set a durability target of 5000 h for fuel cells used in transportation applications [33]. Numerous studies have been reported on the evaluation of planar fuel cells durability [34]–[36]. However, studies on the evaluation of cylindrical PEM fuel cell durability operating in air-breathing mode as well as the development and testing of cylindrical PEM fuel cell stack is very limited.

Performance of air breathing PEMFCs, as explained earlier, depends highly on various factors such as humidity, temperature and flow rates of hydrogen and air. Non-optimal use of such factors can have a significant effect on the life of individual components leading to the timed failure of the cell/stack. The first part of the present study focusses on the evaluation of the durability of a cylindrical PEM fuel cell using the new European driving cycle (NEDC). The second part of the study is dedicated to the development of cylindrical PEM fuel cell stack. The effect of environmental conditions such as humidity and temperature on the performance and endurance of the stack is also presented..

II. Experimental

A. Single cell construction

The construction of a cylindrical PEM fuel cell is explained in our previous study [37]. The individual cell (Diameter: 1.2 cm) used for durability studies had an active area of 6 cm^2 and the cells used for the construction of stack had an active area of 18 cm^2. The commercially available membrane electrode assembly (MEA) (Sainergy Fuel Cell India Pvt. Ltd., India) with Nafion® 212 coated with 0.1 and 0.5 mg/cm^2 of 40% PtC as anode and cathode respectively was used. It was backed with a set of wet proofed carbon cloth (ELAT LT 1400 W) as gas diffusion layer (GDL) for the electrodes.

B. Evaluating the single cell durability

The single cell was placed in an enclosure as shown in Fig. 1. Hydrogen at a flow rate of 200 sccm and air at a flow rate of 500 sccm were supplied to the cell and to the enclosure respectively. Initially, the cell was conditioned for 6 h at a constant current of 1.32 A. Initial polarization curve was then recorded with a cut-off potential of 0.4 V. The durability of the fuel cell was then evaluated using the new European driving cycle (NEDC) as given in Fig. 2 [38]. The maximum load cycling current was chosen to be 0.615 A corresponding to the cell potential of 0.65 V in the initial polarization experiment. In NEDC, the cell must be subjected to 50 consecutive load cycles for a total duration of 16 h. The rest time of 16 h was given after 16 h of load cycling to distinguish between recoverable and irrecoverable potential loss.

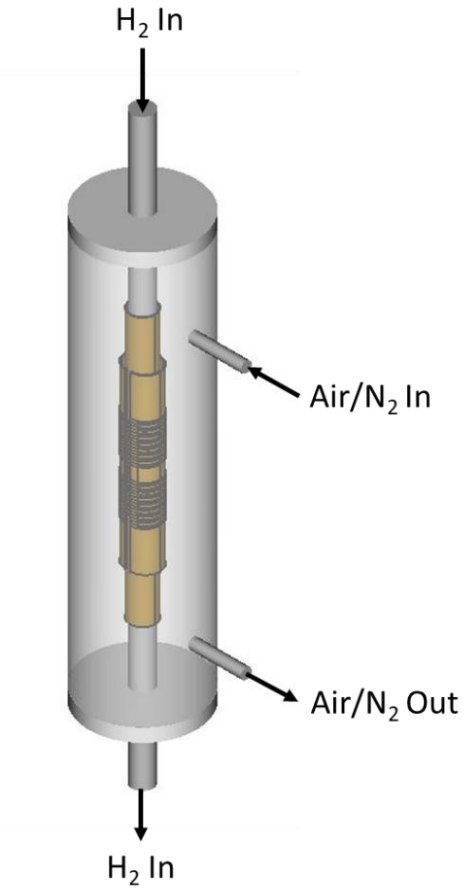

Fig 1. Schematic of the experimental setup used for single cell durability studies

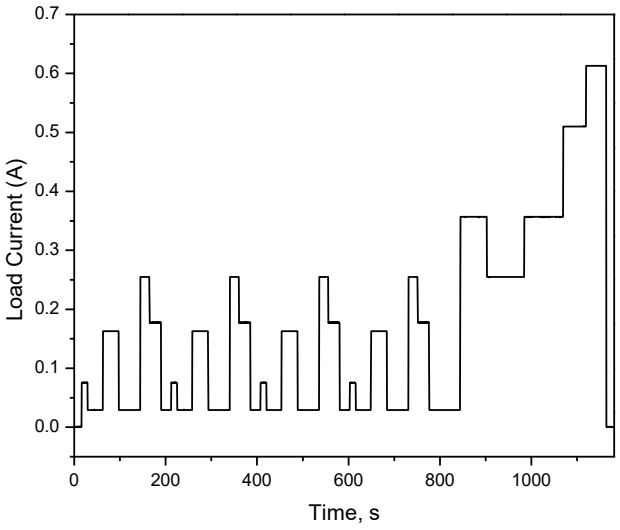

Fig 2. Load cycle profile used to analyze the cylindrical PEM fuel cell durability

The fuel cell was characterized for electrochemically active surface area (ECSA), hydrogen crossover, ohmic resistance, and polarization curve before and after load cycling. ECSA was calculated by performing 5 repeated cycles of cyclic voltammetry (CV) from 0 to 0.8 V at a scan rate of 200 mV/s. The hydrogen crossover measurement was performed by linear sweep voltammetry (LSV) from 0 to 0.8 V at a scan rate of 2 mV/s. The ohmic resistance of the cell was obtained from electrochemical impedance spectroscopy (EIS). The frequency range of 0.1 to 10 kHz was employed for EIS while drawing a constant current of 0.1 A. The root mean square (RMS) value of the current was 0.5 A. The cell was operated at room temperature and the gases supplied to the cell were humidified at room temperature. Air was supplied to the cathode during load cycling, polarization and EIS measurements and was replaced with nitrogen in the same setup during ECSA and hydrogen crossover measurements.

BK precision 8500 DC electronic load was used to apply the dynamic load cycles as well as characterize the cell/stack. Versastat 4 potentiostat/galvanostat system from Princeton Applied Research was used to perform CV, LSV and EIS. Scanning Electron Microscope (SEM) images of the unused MEA and the MEA subjected to load cycling were recorded using JSM-5600LV Microscope with an attached Energy Dispersive X-ray Spectrometer.

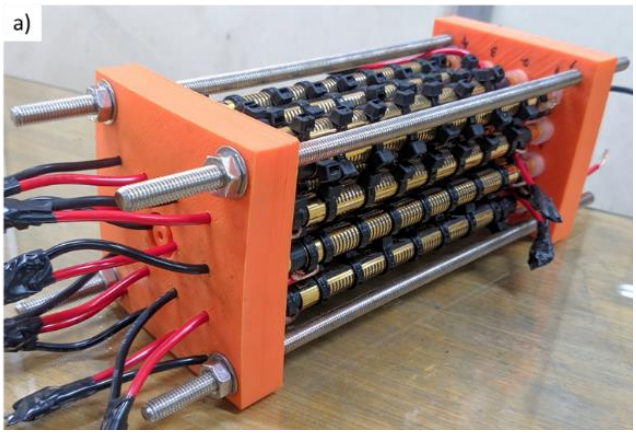

b)

Cell 1	Cell 2	Cell 3	Cell 4
Cell 8	Cell 7	Cell 6	Cell 5
Cell 9	Cell 10	Cell 11	Cell 12
Cell 16	Cell 15	Cell 14	Cell 13

Fig 3. a) The cylindrical fuel cell stack, b) Cells' orientation in the stack

C. Stack construction

The cells used for the stack construction (Fig. 3a) were numbered for identification in terms of the individual performance and were connected in series. A set of 16 cylindrical fuel cells arranged in 4x4 pattern (Fig. 3b) was housed between a set of upper and lower blocks. The blocks had defined pathways to distribute the fuel at the top before entering the cells and collected from the cells at the bottom to be sent out to the atmosphere. The blocks were fabricated using acrylic butadiene styrene (ABS) with Prusa i3 MK3 3D printer. Hydrogen and air were supplied to the setup using a fuel cell test station (Scribner 850e, Virginia). The stack weighed 1.35 kg and had dimensions of 10 x 10 x 21.5 cm^3.

D. Environmental chamber

In order to evaluate the effect of temperature and humidity of the environment, an environmental chamber was fabricated in-house with acrylic sheets (10 mm thickness) (Fig. 4). It had an overall inner dimension as 30 x 30 x 60 cm^3 with diagonally opposite inlet and outlet for air to flow. A fan (6 W) was used to circulate the air inside the chamber for its better distribution. A 400 W heater with a proportional integral derivative (PID) controller was put up near the fan for maintaining the temperature in the chamber at the desired value.

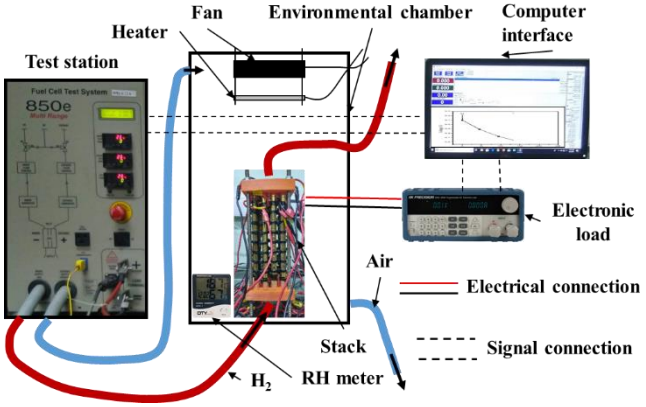

Fig 4. Schematic layout of the experimental setup

E. Environmental setup

The setup consisted of the environmental chamber housing the stack, fan, heater with controller and RH meter (Fig. 4). The stack was supplied with the fuel and oxidant with the help of the test station whereas characterization was done using the electronic load (BK PRECISION model 8500, California) controlled using a computer interface. Hydrogen humidity was maintained at 100% in all the experiments whereas temperature and humidity of air was varied to observe their effect on the performance and endurance of the stack. The polarization curve was obtained in constant current (CC) mode by varying the current from 0 to 2.5 A in steps of 500 mA with one-minute interval between each step. The endurance of the stack was evaluated by measuring the potential when a constant current load of 2 A was applied for two hours. The endurance testing was stopped either at the end of two hours or when the potential of the stack fell below 6 V.

III. RESULTS AND DISCUSSION

A. *Durability of single cell*

The cell potential at three different current densities obtained from the polarization data is given in Fig. 5. The cell potential was always found to be lower at the end of load cycling compared to that at the beginning. However, the decrease in cell potential during the load cycling was recovered after the rest period of 16 h. Such decrease in cell potential during the load cycling could be attributed to the flooding of catalyst layer due to the continuous operation of the cell for 16 h. During the rest period, the excess water present on the cathode surface could have evaporated leading to the increase in cell potential.

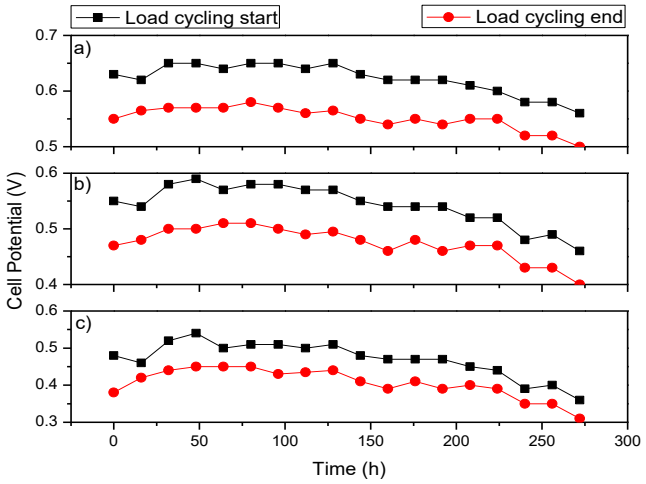

Fig 5. Variation of cell potential with respect to time at current densities of a) 100 mA/cm2, b) 150 mA/cm2 and c) 200 mA/cm2

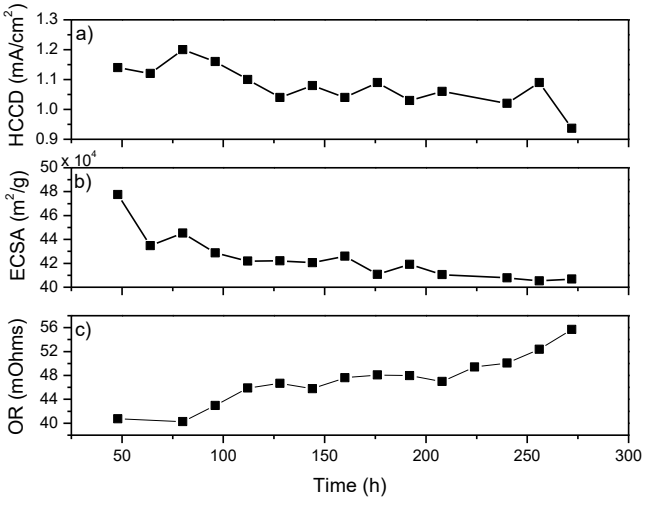

Fig 6. Variation of a) hydrogen crossover current density, b) ECSA and c) ohmic resistance with respect to time

The cell potential at all three current densities improved for the first 48 h followed by a steady decline until 224 h. After 224 h, the rate of degradation was very high, and the average loss in cell potential after 272 h of operation is 16%. The factor corresponding to the faster cell degradation could be elucidated from Fig. 6 which shows the variation of hydrogen crossover current density (HCCD), ECSA and ohmic resistance (OR) with respect to time. There was no appreciable increase in HCCD observed during the entire duration of durability test underlining that the hydrogen crossover was not a contributing factor to the degradation of the cell.

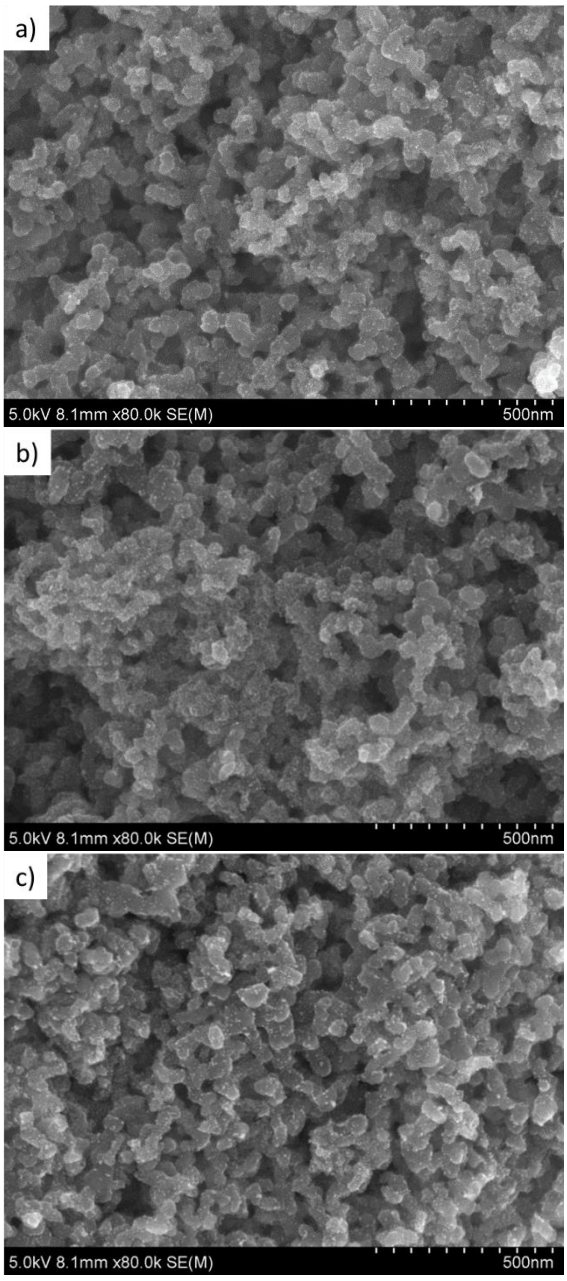

Fig 7. SEM image of (a) unused MEA, (b) anode catalyst layer and (c) cathode catalyst layer of MEA after 272 h of operation

ECSA calculated from the hydrogen adsorption region of the voltammogram followed a steady decrease with time until 208 h. During this period, the ohmic resistance of the cell was observed to increase steadily. However, the decrease in ECSA after 208 h was very minimal however, the increase in ohmic resistance was observed to accelerate. The SEM image of the catalyst layer of an unused MEA and the MEA subjected to durability test is given in Fig. 7. The morphology of the catalyst layer after 272 h of operation was found to be similar to that of the unused catalyst layer. This suggests that the catalyst particles did not undergo any appreciable degradation

like agglomeration or dissolution during the cell operation. Hence, the high rate of performance degradation of the cell after 224 h was not caused by the degradation of catalyst particles but by the increase in ohmic resistance. The increase in ohmic resistance could either be because of irreversible drying of membrane or the corrosion of current collectors.

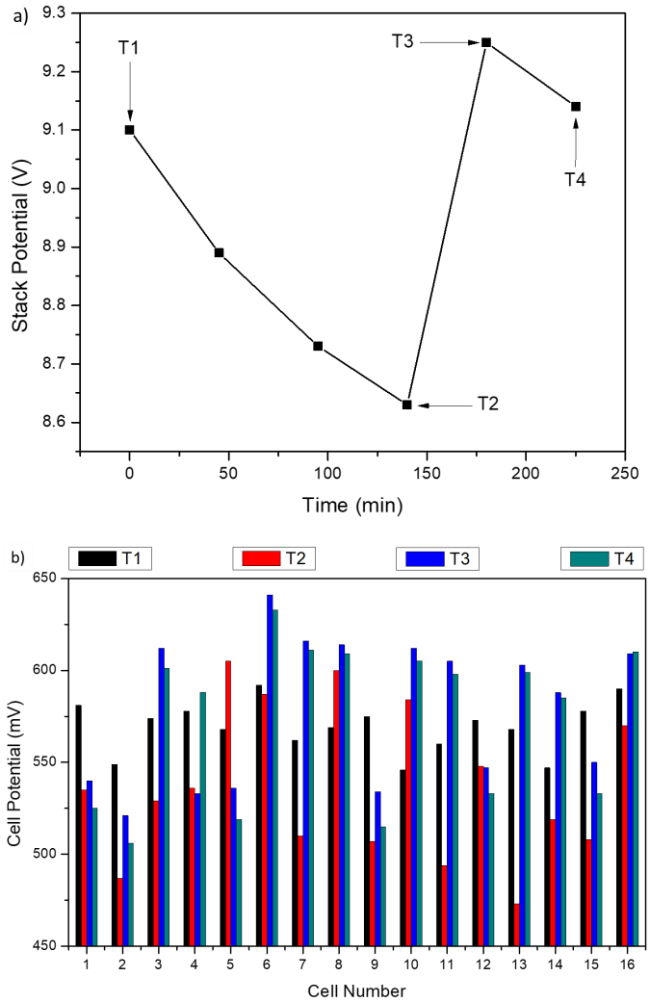

Fig 8. a) Chronopotentiometric analysis of the stack for a constant current of 1 A, b) Changes in the potential of individual cells at different time points

B. *Evaluation of stack performance*

1) Hydrogen humidification temperature

Before studying the effect of ambient air conditions, it was important to standardize the operating conditions of hydrogen. Initially, hydrogen was humidified at 50 °C and supplied to the stack at a flow rate of 3 lpm. A constant current of 1 A was drawn from the stack and the corresponding potential of the stack was measured (Fig. 8a). As observed from the figure, the stack potential was found to decrease over time which added to the measurement of the potential of the individual cells (Fig. 8b). The comparison of potentials of the individual cells at time T1 and T2 underlined that the performance of all the cells was not decreased with the same rate. The potential of the cells 2, 9, 11, 13 and 15 was decreased by more than 50 mV, however, the cells 8 and 10 showed an increment in the performance. The comparison highlighted the fact that the water carried by the hydrogen got condensed in the distribution channels of the flow distribution plate which in turn restricted the access of hydrogen to some of the cells.

Hence, the hydrogen supplied to the stack was humidified only at room temperature resulting in the increment of the stack potential (time T2 to T3, Fig. 4). The potentials of the cells 3, 6, 7, 11 and 13 were found to be higher than the initial ones which could be attributed to the fact that the water carried by the hydrogen was utilized for hydrating the Nafion® membrane which improved the ionic conductivity of the membrane thereby increasing the cell potential. In order to further confirm that the decrease in the voltage was due to the condensation of water in the distribution channels, the heater in the hydrogen humidifier was again switched on and set at 50 °C. This again resulted in decrease in the potential of cells (time T3 and T4). Therefore, hydrogen humidified at room temperature was used in rest of the experiments.

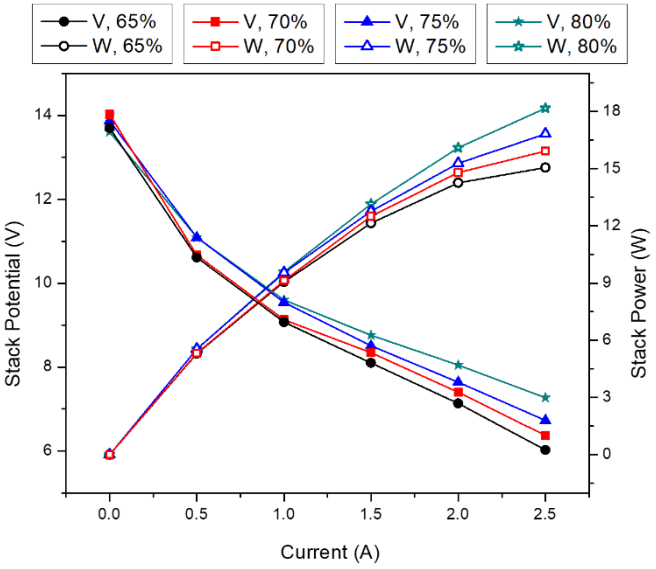

Fig 9. Effect of relative humidity variation of air on the stack performance

2) Relative humidity of air

After identifying the operating conditions on the anode side, the stack was then placed inside the environment chamber to study the effect of RH and temperature of air. The air was supplied to the chamber at a flow rate of 3 lpm. The relative humidity was observed to increase the performance of the stack (Fig. 9). The peak power of the stack was increased from 15 W to 18 W, when the RH of the air increased from 65% to 80%. This increase in peak power could be attributed to the decrease in the ohmic resistance of the stack. At higher RH, the amount of water carried by the air was higher than at a lower RH. Hence, the amount of water which evaporated from the cathode surface to air would be lower at higher RH and vice-versa. The unevaporated water on the cathode surface at higher RH would diffuse back into the membrane thereby increasing its ionic conductivity. The increase in ionic conductivity of the membrane resulted in the decrease in ohmic resistance thereby increasing the peak power of the stack.

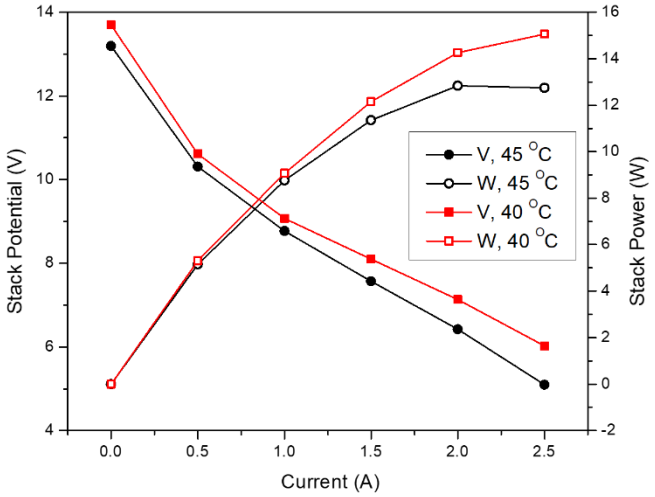

Fig 10. Effect of air temperature on the stack performance

3) Temperature of air

Fig. 10 shows the effect of air temperature on the polarization and power of the stack. The RH of air was found to be constant at 65% and peak power of the stack was observed to decrease from 15 W to ~13 W while the temperature of the air was increased from 40 °C to 45 °C. The amount of water required to maintain a particular RH was higher at higher temperatures. The increase in water evaporation rate from the cathode surface was observed to be the reason behind RH being constant. Such increase in the concentration gradient of water led to the diffusion of water molecules from the membrane to the cathode surface. This in turn resulted in the dehydration of the membrane thereby reducing the peak power of the stack.

4) Stack endurance

The endurance of the stack was studied at different RH and temperatures of air by applying a constant current load of 2 A for a duration of 2 h (Fig. 11). The potential of the stack was observed to deteriorate for 65% RH and 70% RH at a temperature of 40 °C. The rate of such deterioration at 75% RH at 35 °C was comparatively less than that at 70% RH at 40 °C. The amount of water evaporated from the cathode surface was higher at lower RH and at elevated temperatures as discussed earlier. Hence, the gradual decrease in the stack potential was attributed to the membrane drying caused by the above combined effect. However, the stack potential started increasing after a period of 60 minutes for 80% RH at 35 °C. This further established the fact that the membrane hydration was improved at higher RH and at lower temperature due to the back diffusion of water produced at the cathode surface during stack operation. Hence it was essential to maintain high RH and low temperature at the cathode for drawing substantial power from the stack for a longer period of time.

In order to elucidate the effect of cell position within the stack on its performance, the potential distribution of all the cells during the endurance test of the stack at 80% RH and 35 °C is plotted in Fig. 12. The variation in potential among the cells was due to the inherent characteristics of MEAs and their design parameters. The potential of cells 6 and 10 was respectively found to be the highest (~483 mV) and lowest (~400 mV) compared to that of the other cells. Both these cells occupied the inner position in the stack which underlined that they didn't suffer from oxygen deficiency. The performance of an individual cell, therefore, was concluded to be independent of its position within the stack.

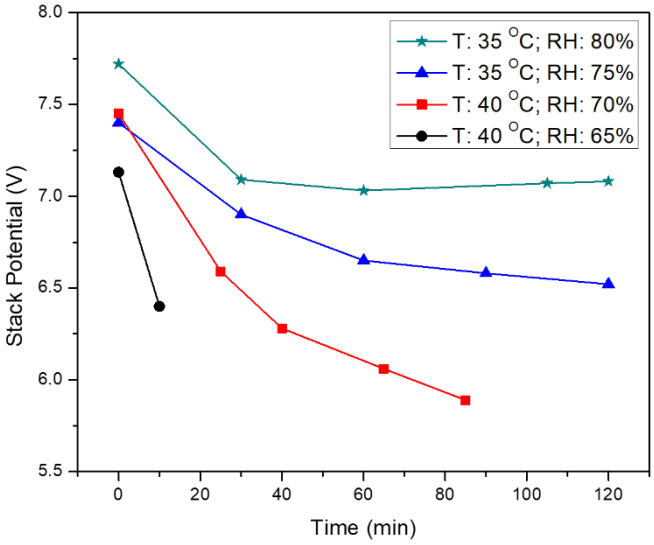

Fig 11. Endurance test of the stack at a constant current of 2 A for different RH and temperature values

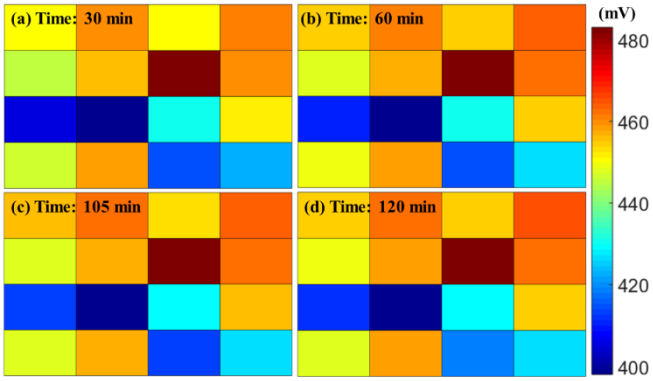

Fig 12. Potential distribution in the stack over time; (a) 30, (b) 60, (c) 105 and (d) 120 min

IV. Conclusions

The present work underlines the performance analysis of a single cylindrical cell at different current densities viz. 100, 150 and 200 mA/cm^2 for more than 250 h. The parameters such as hydrogen crossover, ohmic resistance and electrochemically active surface area that are responsible for the durability and the performance of the cell were evaluated over the timeline. Among all these, ohmic resistance was found to be the major contributor for the decrease in cell potential over time. The repetitive dynamic load cycles could have led to the irreversible drying of the membrane as well as affected the chemical stability of the current collector resulting in a decrease in life of the cell. The effect of relative humidity and temperature of the oxidant i.e. air on the performance and durability of the tubular fuel cell stack

without changing the operational parameters of the fuel supplied was also investigated. To have a better insight of humidity effect, the stack was operated at different RH viz. 65, 70, 75 and 80% keeping the temperature constant. This resulted in the stack performing better with higher RH. The influence of operating temperature of the oxidant was also examined and it followed an inverse trend of performance with temperature. The increase in air temperature (40 to 45 °C) highlighted the effect of dehydration of the membranes thus adding to the ohmic losses. The positioning of cells was also set as a parameter to study its effect on the performance of the stack; however, it played a neutral role in the durability study. Both RH and temperature affected the life of the stack with temperature dominating the effect. Higher RH and lower temperature seemed to be optimized parameters for higher durability of the stack.

Less subsystems in an air breathing fuel cells appear to be attractive for automobile/ autonomous vehicles. It would be beneficial if humidification system can also be eliminated. The use of self-humidifying membranes/MEAs would help address this requirement. It could possibly increase the durability of the stack as well. Future work, therefore, will involve the assessment of self-humidifying MEAs in the stack of cylindrical fuel cells, which is expected to deliver higher volumetric and gravimetric power density by retaining the advantages of an air-breathing stack.

ACKNOWLEDGMENT

The authors of this paper would like to thank Naval Research Board, Defense Research and Development Organization (DRDO), Government of India for financially supporting this work. The authors also extend their thanks to Mr. Vaibhav Verma of Naval Materials Research Laboratory (NMRL) for his help with the experiments.

REFERENCES

[1] T. Bocklisch, "Hybrid energy storage systems for renewable energy applications," *Energy Procedia*, vol. 73, pp. 103–111, 2015, doi: 10.1016/j.egypro.2015.07.582.

[2] M. H. Braga, N. S. Grundish, A. J. Murchison, and J. B. Goodenough, "Alternative strategy for a safe rechargeable battery," *Energy Environ. Sci.*, vol. 10, no. 1, pp. 331–336, 2017, doi: 10.1039/c6ee02888h.

[3] Q. Li, Y. Liu, S. Guo, and H. Zhou, "Solar energy storage in the rechargeable batteries," *Nano Today*, vol. 16. Elsevier B.V., pp. 46–60, Oct. 01, 2017, doi: 10.1016/j.nantod.2017.08.007.

[4] D. E. Eapen, S. R. Choudhury, and R. Rengaswamy, "Low grade heat recovery for power generation through electrochemical route: Vanadium Redox Flow Battery, a case study," *Appl. Surf. Sci.*, vol. 474, pp. 262–268, Apr. 2019, doi: 10.1016/j.apsusc.2018.02.025.

[5] R. Ramkumar and M. Minakshi, "Fabrication of ultrathin CoMoO4 nanosheets modified with chitosan and their improved performance in energy storage device," *Dalt. Trans.*, vol. 44, no. 13, pp. 6158–6168, 2015, doi: 10.1039/c5dt00622h.

[6] S. H. Ahn *et al.*, "Effects of platinum loading on the performance of proton exchange membrane fuel cells with high ionomer content in catalyst layers," *Int. J. Hydrogen Energy*, vol. 38, no. 23, pp. 9826–9834, 2013, doi: 10.1016/j.ijhydene.2013.05.123.

[7] S. M. Andersen and M. J. Larsen, "Performance of the electrode based on silicon carbide supported platinum catalyst for proton exchange membrane fuel cells," *J. Electroanal. Chem.*, vol. 791, pp. 175–184, 2017, doi: 10.1016/j.jelechem.2017.03.018.

[8] A. De Ias Heras, F. J. Vivas, and J. M. Andujar, "From the cell to the stack. A chronological walk through the techniques tomanufacture the PEFCs core," *Renew. Sustain. Energy Rev.*, vol. 96, pp. 29–45, 2018, doi: https://doi.org/10.1016/j.rser.2018.07.036.

[9] Q. Li, W. Yang, F. Li, A. Cui, and J. Hong, "Preparation of CoB/ZIF-8 supported catalyst by single step reduction and its activity in hydrogen production," *Int. J. Hydrogen Energy*, vol. 43, pp. 271–282, 2017, doi: 10.1016/j.ijhydene.2017.11.105.

[10] G. Y. Chen *et al.*, "Gradient design of Pt/C ratio and Nafion content in cathode catalyst layer of PEMFCs," *Int. J. Hydrogen Energy*, pp. 6–11, 2017, doi: 10.1016/j.ijhydene.2017.06.229.

[11] A. C. Bhosale, M. A. Mahajan, and P. C. Ghosh, "Optimization of contact resistance with better gasketing for a unitized regenerative fuel cell," *Int. J. Hydrogen Energy*, vol. 44, no. 37, pp. 20953–20962, 2019, doi: 10.1016/j.ijhydene.2018.09.090.

[12] M. S. Garapati and R. Sundara, "Highly efficient and ORR active platinum-scandium alloy-partially exfoliated carbon nanotubes electrocatalyst for Proton Exchange Membrane Fuel Cell," *Int. J. Hydrogen Energy*, vol. 44, no. 21, pp. 10951–10963, Apr. 2019, doi: 10.1016/j.ijhydene.2019.02.161.

[13] R. Nayak, M. Sundarraman, P. C. Ghosh, and A. R. Bhattacharyya, "Doped poly (2, 5-benzimidazole) membranes for high temperature polymer electrolyte fuel cell: Influence of various solvents during membrane casting on the fuel cell performance," *Eur. Polym. J.*, vol. 100, no. August 2017, pp. 111–120, 2018, doi: 10.1016/j.eurpolymj.2017.08.026.

[14] N. Shaari and S. K. Kamarudin, "Graphene in electrocatalyst and proton conductiong membrane in fuel cellapplications: An overview," *Renew. Sustain. Energy Rev.*, vol. 69, pp. 562–870, 2017, doi: http://dx.doi.org/10.1016/j.rser.2016.07.044.

[15] J. Wang, "Theory and practice of flow field designs for fuel cell scaling-up: A critical review," *Appl. Energy*, vol. 157, pp. 640–663, 2015, doi: 10.1016/j.apenergy.2015.01.032.

[16] A. C. Bhosale, S. R. Mane, D. Singdeo, and P. C. Ghosh, "Modeling and experimental validation of a unitized regenerative fuel cell in electrolysis mode of operation," *Energy*, vol. 121, pp. 256–263, 2017, doi: http://dx.doi.org/10.1016/j.energy.2017.01.031.

[17] J. Dillet *et al.*, "Impact of flow rates and electrode specifications on degradations during repeated startups and shutdowns in polymer-electrolyte membrane fuel cells," *J. Power Sources*, vol. 250, pp. 68–79, 2014, doi: 10.1016/j.jpowsour.2013.10.141.

[18] A. C. Bhosale, S. Meenakshi, and P. C. Ghosh, "Root cause analysis of the degradation in a unitized regenerative fuel cell," *J. Power Sources*, vol. 343, pp. 275–283, 2017, doi: 10.1016/j.jpowsour.2017.01.060.

[19] Y. Devrim, H. Devrim, and I. Eroglu, "Development of 500 W PEM fuel cell stack for portable power generators," *Int. J. Hydrogen Energy*, vol. 40, pp. 7707–7719, 2015, doi: doi.org/10.1016/j.injydene.2015.02.005.

[20] G. Giacoppo, S. Hovland, and O. Barbera, "2 kW Modular PEM fuel cell stack for space appliations: Development and test for opeation under relevant conditions," *Appl. Energy*, vol. 242, pp. 1683–1696, 2019, doi: doi,org/10.1016/j.apenergy.2019.03.188.

[21] I. Han, B.-K. Kho, and S. Cho, "Development of a polymer electrolyte membrane fuel cell stack for an underwater vehicle," *J. Power Sources*, vol. 304, pp. 244–254, 2016, doi: dx.doi.org/10.1016/j.jpowsour.2015.11.049.

[22] P. Corbo, F. Migliardini, and O. Veneri, "Performance investigation of 2.4kW PEM fuel cell stack in vehicles," *Int. J. Hydrogen Energy*, vol. 32, no. 17, pp. 4340–4349, 2007, doi: 10.1016/j.ijhydene.2007.05.043.

[23] N. Bussayajarn, H. Ming, K. K. Hoong, W. Y. Ming Stephen, and C. S. Hwa, "Planar air breathing PEMFC with self-humidifying MEA and open cathode geometry design for portable applications," *Int. J. Hydrogen Energy*, vol. 34, no. 18, pp. 7761–7767, 2009, doi: 10.1016/j.ijhydene.2009.07.077.

[24] T. Zeng *et al.*, "Experimental investigation on the mechanism of variable fan speed control in Open cathode PEM fuel cell," *Int. J. Hydrogen Energy*, Aug. 2019, doi: 10.1016/J.IJHYDENE.2019.07.119.

[25] D. Chu and R. Jiang, "Performance of polymer electrolyte membrane fuel cell (PEMFC) stacks: Part I. Evaluation and simulation of an air-breathing PEMFC stack," *J. Power Sources*, vol. 83, no. 1, pp. 128–133, 1999, doi: 10.1016/S0378-7753(99)00285-2.

[26] T. Fabian *et al.*, "The role of ambient conditions on the performance of a planar, air-breathing hydrogen PEM fuel cell," *J. Power Sources*, vol. 161, no. 1, pp. 168–182, Oct. 2006, doi: 10.1016/j.jpowsour.2006.03.054.

[27] K. S. Dhathathreyan, N. Rajalakshmi, K. Jayakumar, and S. Pandian, "Forced Air-Breathing PEMFC Stacks," *Int. J. Electrochem.*, vol. 2012, pp. 1–7, 2012, doi: 10.1155/2012/216494.

[28] D. SANTAROSA, D. PINTO, V. SILVA, R. SILVA, and C. RANGEL, "High performance PEMFC stack with open-cathode at ambient pressure and temperature conditions," *Int. J. Hydrogen Energy*, vol. 32, no. 17, pp. 4350–4357, Dec. 2007, doi: 10.1016/j.ijhydene.2007.05.042.

[29] S. R. Suseendiran, S. Pearn-Rowe, and R. Rengaswamy, "Strategies for Effective Utilization of Hydrogen in Cylindrical PEM Fuel Cells," *ECS Trans.*, vol. 80, no. 8, pp. 485–496, Aug. 2017, Accessed: Dec. 13, 2017. [Online]. Available: http://ecst.ecsdl.org/lookup/doi/10.1149/08008.0485ecst.

[30] B. Bullecks, R. Rengaswamy, D. Bhattacharyya, and G. Campbell, "Development of a cylindrical PEM fuel cell," *Int. J. Hydrogen Energy*, vol. 36, no. 1, pp. 713–719, 2011.

[31] J. M. Sierra, S. J. Figueroa-Ramirez, S. E. Diaz, J. Vargas, and P. J. Sebastian, "Numerical evaluation of a PEM fuel cell with conventional flow fields adapted to tubular plates," *Int. J. Hydrogen Energy*, vol. 39, pp. 16694–16705, 2014, doi: doi.org/10.1016/j.ijhydene.2014.04.078.

[32] Z. Saghali and J. Mahmoudimehr, "Superiority of a novel conic tubular PEM fuel cell over the conventional cylindrical one," *Int. J. Hydrogen Energy*, vol. 42, pp. 28865–28882, 2017, doi: doi.org/10.1016/j.ijhydene.2017.10.058.

[33] U. S. Drive, "Fuel Cell Technical Team Roadmap," 2017. [Online]. Available: https://www.energy.gov/sites/prod/files/2017/11/f46/FCTT_Roadmap_Nov_2017_FINAL.pdf.

[34] R. Lin, B. Li, Y. P. Hou, and J. M. Ma, "Investigation of dynamic driving cycle effect on performance degradation and micro-structure change of PEM fuel cell," *Int. J. Hydrogen Energy*, vol. 34, no. 5, pp. 2369–2376, Mar. 2009, doi: 10.1016/J.IJHYDENE.2008.10.054.

[35] A. Bose, P. Babburi, R. Kumar, D. Myers, J. Mawdsley, and J. Milhuff, "Performance of individual cells in polymer electrolyte membrane fuel cell stack under-load cycling conditions," *J. Power Sources*, vol. 243, pp. 964–972, Dec. 2013, doi: 10.1016/J.JPOWSOUR.2013.05.156.

[36] F. Wang *et al.*, "Investigation of the recoverable degradation of PEM fuel cell operated under drive cycle and different humidities," *Int. J. Hydrogen Energy*, vol. 39, no. 26, pp. 14441–14447, Sep. 2014, doi: 10.1016/J.IJHYDENE.2014.02.023.

[37] S. R. Suseendiran, S. Pearn-Rowe, and R. Rengaswamy, "Development of cylindrical PEM fuel cells with semi-cylindrical cathode current collectors," *Int. J. Hydrogen Energy*, 2019, doi: https://doi.org/10.1016/j.ijhydene.2019.09.113.

[38] G. Tsotridis, A. Pilenga, G. De Marco, and T. Malkow, *EU Harmonised Test Protocols for PEMFC MEA Testing in Single Cell Configuration for Automotive Applications; JRC Science for Policy report*. 2015.